Kinetics of the Reaction of CH_3S with Unsaturated Hydrocarbons

R. Jeffrey Balla,† Brad R. Weiner,† and H. H. Nelson*

Contribution from the Chemistry Division, Code 6111, Naval Research Laboratory, Washington, DC 20375-5000. *Received November 21, 1986*

Abstract: The reactions of the methyl thiyl radical, CH_3S, with 1,3-butadiene and allene have been studied as a function of temperature (296–455 K) and pressure (20–60 Torr) by using laser-induced fluorescence (LIF) as a kinetic probe. The CH_3S radical adds to 1,3-butadiene to form an adduct. At higher temperatures, an equilibrium was observed, and the approach of the CH_3S radical to its equilibrium concentration was monitored in real time experiments. These data produce equilibrium constants for a range of temperatures. Arrhenius parameters for the forward reaction, $k(\pm 2\sigma) = (4.5 \pm 1.3) \times 10^{-13} \exp[(0.60 \pm 0.21 \text{ kcal/mol})/RT]$ cm^3/s, and the reverse reaction, $k(\pm 2\sigma) = (3.7 \pm 22) \times 10^{+13} \exp[(-18.4 \pm 4.6 \text{ kcal/mol})/RT]$ s^{-1}, have also been obtained. Thermodynamic values for the reaction of CH_3S with 1,3-butadiene ($\Delta S°_T = -29.7 \pm 8.6$ cal/mol K; $\Delta H°_T = -18.7 \pm 3.3$ kcal/mol; where the errors represent $\pm 2\sigma$) were determined by using a second law procedure. The curved Arrhenius plot for the reaction of CH_3S with allene was fit to the sum of two Arrhenius expressions $k(\pm 2\sigma) = (3.2 \pm 24) \times 10^{-11} \exp[(-7.2 \pm 8.2 \text{ kcal/mol})/RT] + (6.7 \pm 30) \times 10^{-16} \exp[(+1.3 \pm 2.6 \text{ kcal/mol})/RT]$ cm^3/s indicating that at least two different reaction channels are occurring over the temperature range studied. Possible mechanisms for the reactions are discussed. Rate constants for the room temperature reaction of CH_3S with ethylene and propylene as well as upper limits for the reactions with *cis*-2-butene, acetylene, and methyl acetylene were also measured.

Organosulfur compounds occur naturally in most crude fuels as well as in many synthetic fuels. Processing and combustion of these fuels produce alkyl thiyl radicals, which may in turn play a role in the subsequent chemistry.[1] Little experimental data exist concerning the reactivity of alkyl thiyl radicals. Small concentrations of these species have been shown to have a marked effect on the atmospheric sulfur cycle.[2] Alkyl thiyl radical reactivity warrants further investigation to help develop accurate models for both atmospheric and combustion chemistry.

The known chemistry of these species has been reviewed recently.[3] Most studies of these radicals have relied on product analysis techniques to obtain relative rate constants. Absolute rate constants have been reported for reactions of the HS radical.[4-6] Recent published data on the electronic spectroscopy of CH_3S ($A^2A_1 \leftarrow X^2E_{3/2,1/2}$) provide the groundwork for kinetic studies.[7,8] Absolute rate constants for the reaction of CH_3S with NO, NO_2, and O_2[9] and an upper limit for the reaction with O_3[10] have been reported. Since the rate coefficients for reactions of both HS[6] and CH_3S[9] with O_2 are $\leq 2 \times 10^{-17}$ cm^3/s, it is important to measure the rate constants for the reaction of alkyl thiyl radicals with other species.

Previous experiments on the reactions of alkyl thiyl radicals with alkenes and alkynes suggest reversible adduct formation as the primary process.[11-16] For example, isomerization of *cis*-2-butene to *trans*-2-butene proceeds when CH_3S is present in catalytic amounts in the system.[11,12] In cases where these reactions have been studied over wide temperature ranges, alkyl thiyl radicals have been observed to both add to alkenes at low temperatures and abstract from them at high temperatures.[17]

We report here absolute rate constants for the room temperature reaction of CH_3S with ethylene, propylene, 1,3-butadiene, and allene, by using laser-induced fluorescence (LIF) of the reactant radical as a probe. The kinetics of the reactions of CH_3S with 1,3-butadiene and allene were further investigated as a function of temperature. These data yield a direct measure of the entropy and enthalpy changes for the reaction of CH_3S with 1,3-butadiene as well as the Arrhenius parameters for both reactant molecules. We have also determined upper limits for the absolute rate constants in the reactions of CH_3S with acetylene, methyl acetylene, *cis*-2-butene, isobutane, and ammonia.

Experimental Section

The apparatus has been described in detail previously.[18] In brief, methyl thiyl radicals, CH_3S, are produced by pulsed photolysis of dimethyl disulfide, $(CH_3S)_2$, by using the frequency quadrupled output (266 nm; ca. 75 mJ/cm^2) of a Quantel Model 481C Nd:YAG laser. The CH_3S concentration is probed by monitoring the total fluorescence resulting from laser excitation of the $A^2A_1 \leftarrow X^2E$ transition near 371.8 nm with a Lambda Physik FL2002 dye laser pumped by a rare gas halide excimer laser (Lambda Physik EMG 102) by using the dye QU1 (Lambda Physik; LC3690). The pump and probe laser beams counterpropagate collinearly through the reaction cell which consists of a 5-cm diameter stainless-steel cross. The cell is contained in a forced-convection oven equipped with ports for the laser beams and light collection optics. Oven temperatures are constant to ±1 K. A photomultiplier tube (RCA 31000) collects collimated emission through a series of discrimination filters (450-nm band-pass dielectric; 1-cm path liquid CS_2) at a right angle with respect to the laser beams. Signals from the photomultiplier tube are sampled by a gated integrator and digitized and processed by a microcomputer. Variable delay times between the firing of the photolysis laser and the dye laser are also computer-controlled. In these experiments, the delay time is scanned from 30 μs before and from 20 μs to 5 ms after the photolysis laser pulse. By using this arrangement, we obtain the true base line as well as avoid effects due to vibrational relaxation and prompt emission of photolysis products.

† NRC/NRL Postdoctoral Research Associate.

(1) (a) Daum, K. A.; Massoglia, M. F.; Shendrika, A. D. *J. Air Pollution Control Assoc.* **1982**, *32*, 391. (b) Gehrs, C. W.; Shrimer, D. S.; Herbes, S. E.; Salmon, E. J.; Perry, H. *Chemistry of Coal Utilization*, Elliott, M. A., Ed.; Wiley: New York, 1981; Suppl. Vol. 2, pp 2159–2233.
(2) (a) Hatakeyama, S.; Okuda, M.; Akimoto, H. *Geophys. Res. Lett.* **1982**, *9*, 583. (b) Hatakeyama, S.; Akimoto, H. *J. Phys. Chem.* **1983**, *87*, 2387. (c) Grosjean, D.; Lewis, R. *Geophys. Res. Lett.* **1982**, *9*, 1203.
(3) Heicklen, J. *Rev. Chem. Intermed.* **1985**, *6*, 175.
(4) Black, G. *J. Chem. Phys.* **1984**, *80*, 1103.
(5) Black, G.; Patrick, R.; Jusinski, L. E.; Slanger, T. G. *J. Chem. Phys.* **1984**, *80*, 4065.
(6) Friedl, R. R.; Brune, W. H.; Anderson, J. G. *J. Phys. Chem.* **1985**, *89*, 5505.
(7) Ohbayashi, K.; Akimoto, H.; Tanaka, I. *Chem. Phys. Lett.* **1977**, *52*, 47.
(8) Suzuki, M.; Inoue, G.; Akimoto, H. *J. Chem. Phys.* **1984**, *81*, 5405.
(9) Balla, R. J.; Nelson, H. H.; McDonald, J. R. *Chem. Phys.* **1986**, *109*, 101.
(10) Black, G.; Jusinski, L. E. *J. Chem. Soc., Faraday Trans. 2*, in press.
(11) Walling, C.; Helmreich, W. *J. Am. Chem. Soc.* **1959**, *81*, 1144.
(12) Graham, D. M.; Mieville, R. L.; Sivertz, C. *Can. J. Chem.* **1964**, *42*, 2239.
(13) Graham, D. M.; Soltys, J. F. *Can. J. Chem.* **1969**, *47*, 2719.
(14) Graham, D. M.; Soltys, J. F. *Can. J. Chem.* **1969**, *47*, 2529.
(15) Oswald, A. A.; Griesbaum, K.; Thaler, W. A.; Hudson, B. E., Jr. *J. Am. Chem. Soc.* **1962**, *84*, 3897.
(16) Graham, D. M.; Mieville, R. L.; Pallen, R. H.; Sivertz, C. *Can. J. Chem.* **1964**, *42*, 2250.
(17) Lunazzi, L.; Placucci, G.; Grossi, L. *J. Chem. Soc., Perkin Trans. 2* **1981**, 703.
(18) Balla, R. J.; Nelson, H. H.; McDonald, J. R. *Chem. Phys.* **1985**, *99*, 323.

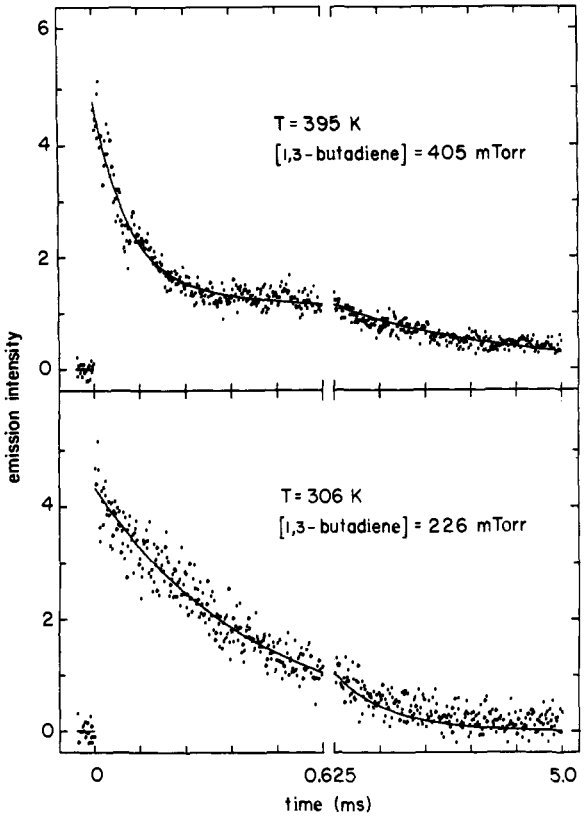

Figure 1. Plots of fluorescence intensity from CH_3S as a function of the delay time between the photolysis and probe lasers. Note the time scale change at the midpoint of the plots. The points are actual experimental data, while the solid lines are the nonlinear least-squares fits to the decays. The lower panel is characterized by a single exponential decay, and the upper panel shows the approach to equilibrium (see text for full explanation).

Experiments are performed under pseudo-first-order conditions. In the absence of any reactant, methyl thiyl radicals decay via self-reaction and diffusion out of the probe beam. Metered flows of dimethyl disulfide, reactants, and buffer gas are combined and flow together through the cell at total flow rates of approximately 0.5 standard L/min. All component gases in the experiment are combined at a distance from the cell which ensures uniform mixing (mixing time ca. 0.25 s). Typical reactant pressures are 0.4–2.0 mTorr $(CH_3S)_2$, 0–600 mTorr (1,3-butadiene), and 0–7 Torr (allene, ethylene, propylene, *cis*-2-butene, isobutane, acetylene, methyl acetylene, and ammonia). Experiments are performed at 20–60 Torr total pressure by using N_2 as a buffer gas.

The dimethyl disulfide (Eastman Kodak, 97% minimum purity) and N_2 (Air Products, 99.998%) are used without further purification. Matheson 1,3-butadiene (C.P. grade, 99%), allene (93% minimum purity liquid phase), ethylene (C.P. grade, 99.5%), propylene (C.P. grade, 99.6%), methyl acetylene (98%), isobutane (99% liquid phase), *cis*-2-butene (95% liquid phase), and ammonia (99.99%) are also used without further purification. Acetylene (Matheson, 99.6%) was passed over silica gel maintained at dry ice temperature to remove any acetone present.

Results

Dimethyl disulfide, $(CH_3S)_2$, was chosen as the photolytic precursor, because it is a clean source of CH_3S radicals and produces no other observable decomposition channels.[19] Other possible precursors, such as CH_3SH or CH_3SCH_3, produce H atoms or alkyl radicals which can complicate the kinetic system. In the absence of added reactant, the CH_3S radicals decay via self-reaction and diffusion. Because of the slow reaction of CH_3S with alkenes, we keep the precursor concentration as low as possible to minimize the contribution of radical self-reaction.

Pseudo-first-order rates for the reaction of CH_3S with alkenes were obtained from plots of the LIF intensity vs. the delay time between the photolysis and probe lasers. Typical data are shown in Figure 1. In experiments carried out at room temperature,

(19) Balla, R. J.; Heicklen, J. *Can. J. Chem.* **1984**, *62*, 162.

Table I. Rate Constants for the Reaction of CH_3S with 1,3-Butadiene[a]

T, K	$k_1 \times 10^{13}$, cm^3/s	$k_{-1} \times 10^{-2}$, s^{-1}	$K_P \times 10^{-3}$, atm^{-1} (ln K_P)	ln K_P + "corrections"
302	11.7 ± 1.0			
306	13.7 ± 1.4			
334	9.6 ± 1.0			
352	9.6 ± 1.3			
352	11.3 ± 1.0			
372	10.4 ± 1.4	6.7 ± 5.0	30 ± 28 (10.3)	10.3
377	9.7 ± 0.5			
384	8.2 ± 1.0	11.7 ± 3.2	13.4 ± 5.4 (9.5)	9.5
393	10.2 ± 1.4			
395	11.1 ± 1.0	30.8 ± 19.4	6.7 ± 4.8 (8.8)	8.8
407	9.2 ± 1.2	51.1 ± 22	3.2 ± 1.8 (8.1)	8.1
419	7.9 ± 3.3	84.0 ± 54	1.6 ± 1.8 (7.4)	7.3

[a] All uncertainties are $\pm 2\sigma$ and are statistical only.

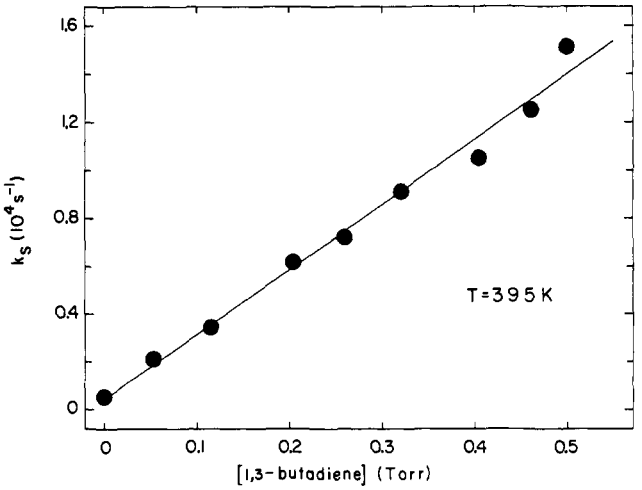

Figure 2. Plot of the pseudo-first-order rate constant vs. 1,3-butadiene pressure. The rate constants were extracted from decays similar to the upper panel in Figure 1.

the CH_3S disappearance in the presence of a reactant was fit to a single exponential decay extending over more than 2 lifetimes (see bottom panel Figure 1). The total pressure was kept constant by using N_2 as a buffer gas, and the CH_3S decay was monitored over a range of reactant pressures. Second-order rate constants result from the slope of a plot of pseudo-first-order rates as a function of reactant pressure.

Reaction of CH_3S with 1,3-Butadiene. For the reaction of CH_3S with 1,3-butadiene in the temperature range 296–333 K, plots of fluorescence intensity vs. delay time can be adequately fit by a single exponential decay, as shown in the bottom panel of Figure 1. Second-order rate constants for the reaction (see Table I) were obtained by using the procedure described above. At higher temperatures (333–410 K), we find that the fluorescence decay is best fit by using the biexponential function

$$\text{signal} = A_S \exp(-k_S t) + A_L \exp(-k_L t) + \text{base line} \quad (1)$$

where A_S, A_L, k_S, and k_L are the adjustable parameters in a nonlinear least-squares fitting routine. Figure 1 (top panel) shows typical data collected in this temperature range along with the best fit (solid line). Varying the 1,3-butadiene concentration showed that k_S depended linearly (see Figure 2) on added reactant. Furthermore, k_L was independent of 1,3-butadiene concentration and was a constant value consistent with the rate of diffusion out of the probe beam.

Assume that CH_3S adds reversibly to 1,3-butadiene until equilibrium is established

$$CH_3S + H_2C{=}CH{-}CH{=}CH_2 \underset{k_{-1}}{\overset{k_1}{\rightleftharpoons}} \text{adduct} \quad (2)$$

where k_1 and k_{-1} are rate constants for the adduct formation and decomposition, respectively. Following the treatment of Ruiz et

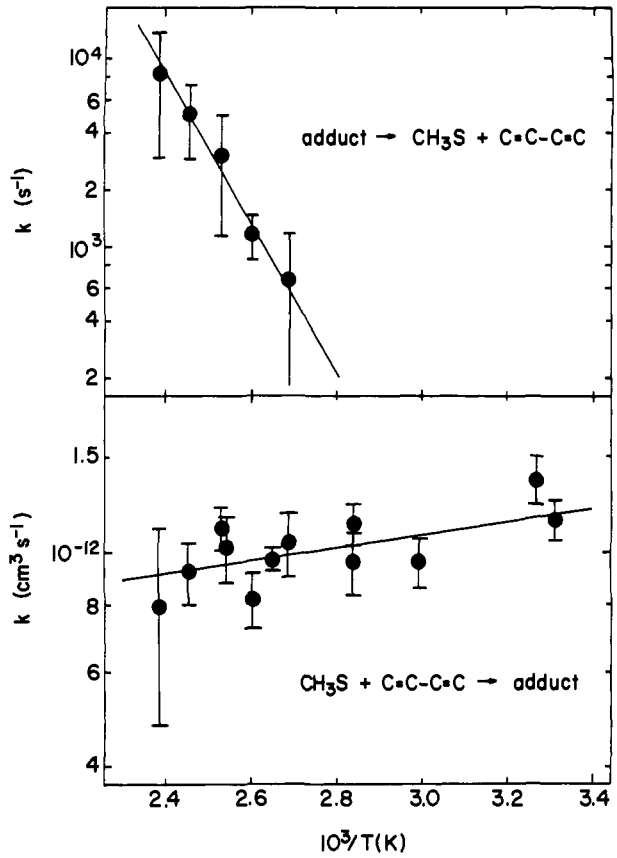

Figure 3. Arrhenius plots for the forward and reverse reactions shown in eq 2 (see text). (●) are actual data points, while the solid line is a linear least-squares fit to the data. Uncertainties are $\pm 2\sigma$.

al.[20] and assuming that CH_3S and the adduct diffuse from the viewing region at the same rate, the observed rate of disappearance of CH_3S at short times, k_S, is

$$k_S = k_1[C_4H_6] + k_{-1} + k_L \quad (3)$$

By using our best fit parameters A_S and A_L and k_1 (the slope of k_S vs. $[C_4H_6]$), we can solve for K_P, the equilibrium constant, and k_{-1}

$$K_P = A_S/A_L[C_4H_6] = k_1/k_{-1} \quad (4)$$

The values of k_1, k_{-1}, and K_P are summarized in Table I for all the temperatures investigated.

Care was taken to assure the validity of the equilibrium constants measured. At temperatures where equilibrium was observed, the mean errors in A_S and A_L were below 10% and under all conditions, $k_1 > 5k_{-1}$. Experiments were performed to test the dependence of the measured equilibrium values on the total pressure and the CH_3S and butadiene concentrations. Both the total pressure and CH_3S concentration were varied by a factor of 2, while the butadiene concentration was varied by almost a factor of ten. Under all conditions, the measured equilibrium constants were independent of these variables.

The rate constants for the forward and reverse reactions (see eq 2) as a function of temperature are plotted in Arrhenius form in Figure 3. The Arrhenius expressions that result are $k_1(\pm 2\sigma) = (4.5 \pm 1.3) \times 10^{-13} \exp[(0.60 \pm 0.21 \text{ kcal/mol})/RT]$ cm^3/s and $k_{-1}(\pm 2\sigma) = (3.7 \pm 22) \times 10^{+13} \exp[(-18.4 \pm 4.6 \text{ kcal/mol})/RT]$ s^{-1} where the uncertainties are statistical only.

Reactions of CH_3S with Allene. As with 1,3-butadiene, the disappearance of CH_3S due to reaction with allene was measured over an extended temperature range (296–455 K). The decay profile in all cases could be fit by a single exponential, extending over at least two reaction lifetimes. Second-order rate constants for the reaction were determined as before by plotting the pseudo-first-order rates as a function of reactant pressure. These data are listed in Table II for all the temperatures investigated and are plotted in Arrhenius form in Figure 4. The curved Arrhenius plot can be fit to the sum of two exponentials, $k(T) = A_1 \exp(-B_1/T) + A_2 \exp(+B_2/T)$ by using a nonlinear least-squares fitting procedure, which best correlates with $k(\pm 2\sigma) = (3.2 \pm 24) \times 10^{-11} \exp[(-7.2 \pm 8.2) \text{ kcal/mol}/RT] + (6.7 \pm 30) \times 10^{-16} \exp[(1.3 \pm 2.6) \text{ kcal/mol}/RT]$ cm^3/s.

Attempts were made to extend the temperature range to ca. 500 K, but the decay of the CH_3S signal was found to be strictly due to diffusion. We believe this results from the rapid dimerization of allene at these elevated temperatures.[21]

Reactions of CH_3S with Other Alkenes. Rate constants for the reaction of CH_3S with ethylene and propylene have also been measured at room temperature, yielding $(2.8 \pm 1.4) \times 10^{-15}$ and $(10 \pm 4) \times 10^{-15}$ cm^3/s, respectively. Both of these small olefins react slowly with CH_3S and quench the fluorescence signal when higher reactant pressures are used. These constraints made accurate rate measurements difficult, and therefore temperature studies of the kinetics were not pursued. Several other molecules (acetylene, methyl acetylene, *cis*-2-butene, isobutane, and ammonia) were tried as possible reactants with CH_3S, but due to the slow rate of these reactions, we were not able to reliably distinguish between reaction and diffusion out of the probe beam. As a result, upper limits for these reaction rates have been set.

Table II. Measured Rate Constants for the Reaction of CH_3S with Allene

T, K	$k(\pm 2\sigma) \times 10^{15}$, cm^3/s	T, K	$k(\pm 2\sigma) \times 10^{15}$, cm^3/s
296	5.7 ± 0.8	352	5.6 ± 1.9
296	6.2 ± 0.8	357	4.4 ± 1.8
297	7.3 ± 1.6	373	4.3 ± 1.2
297	7.5 ± 1.2	407	7.8 ± 0.5
301	5.7 ± 1.2	438	12 ± 2
304	7.1 ± 0.8	452	17 ± 4
313	5.4 ± 0.8	455	16 ± 2
335	7.0 ± 1.2		

Table III. Rate Constants for CH_3S Reactions[a]

reactant	$10^{15}k(298)$, cm^3/s	reactant	$10^{15}k(298)$, cm^3/s
C_2H_4	2.8 ± 1.4	$(CH_3)_3CH$	<3
C_3H_6	10 ± 4	*cis*-CH_3-CH=CH-CH_3	<5.5
C_2H_2	<2	NH_3	<1
$CH_3C{\equiv}CH$	≤6		

[a] All uncertainties are $\pm 2\sigma$.

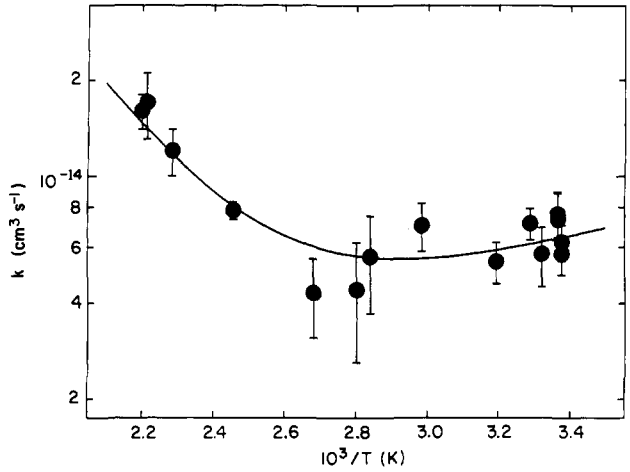

Figure 4. Arrhenius plot for the reaction of CH_3S with allene. The experimental data, (●), are fit to the sum of two Arrhenius expressions, shown as a solid line. Uncertainties are $\pm 2\sigma$.

(20) Ruiz, R. P.; Bayes, K. D.; MacPherson, M. T.; Pilling, M. J. *J. Phys. Chem.* **1981**, *85*, 1622.

(21) Blomquist, A. T.; Verdol, J. A. *J. Am. Chem. Soc.* **1956**, *78*, 109.

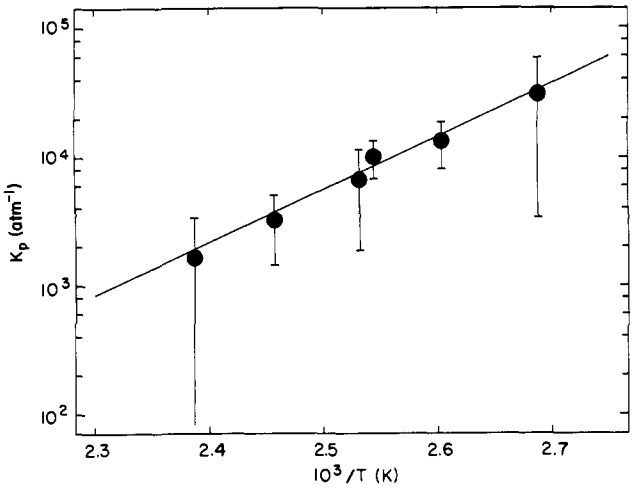

Figure 5. Measured equilibrium constants, K_P, plotted as a function of temperature, (●), for the reaction of CH_3S with 1,3-butadiene. The solid line is a linear least-squares fit to the data points. Uncertainties are $\pm 2\sigma$.

These results are summarized in Table III.

Several other conjugated olefins, e.g., cyclopentadiene and hexatriene, were tried as reactants, but the results were complicated by absorption of the 266-nm light by these species. Most likely, these species fragmented after absorbing a photon, yielding more radicals, thus complicating the kinetics.

Discussion

Thermodynamic information about reaction 2 can be extracted from our equilibrium data. Assuming no heat capacity change for reaction 2 the simplest approach is to use the Van't Hoff equation

$$-\Delta G_T^\circ/RT = \ln K_P = -\Delta H_T^\circ/RT + \Delta S_T^\circ/T \quad (5)$$

Figure 5 shows our data plotted in this form, resulting in $\Delta H_T^\circ = -18.7 \pm 3.3$ kcal/mol and $\Delta S_T^\circ = -29.7 \pm 8.5$ eu taken from the best fit linear least-squares slope and intercept, respectively. The uncertainties represent $\pm 2\sigma$ and result from the propagation of statistical errors from the fitted parameters to the derived equilibrium constants to the thermodynamic constants.

Since the temperature range (374–419 K) over which we were able to accurately measure K_P was somewhat limited, we have employed a third law analysis, to further evaluate our measurements.[22] The third law analysis makes use of calculated entropies to help obtain enthalpy information. This requires knowledge of the temperature variation of the standard molar heat capacity, $(\Delta C_P^\circ(T))$, for the species in reaction 2.[23] The modified Van't Hoff equation can be expressed by

$$\ln K_P + \text{"corrections"} = \Delta S^\circ_{298}/R - \Delta H^\circ_{298}/RT \quad (6)$$

where "corrections" $= a[(T - 298)/T - \ln T/298]/R - b(T - 298)^2/2RT - c(T - 298)^2(T + 2(298))/6RT$. Entropy changes $(\Delta S^\circ_{298} = -30.5$ cal/mol K) for reaction 2 were obtained by using group additivity methods,[24,25] assuming that the adduct was formed by addition to the terminal carbon of 1,3-butadiene. The plot obtained from the third law analysis is shown in Figure 6, and values for $\ln K_p$ + "corrections" are presented in Table I. The corrections had a small effect, changing $\ln K_p$ by less than 1% and yielding $\Delta H^\circ_{298} = -19.0 \pm 0.6$ kcal/mol for reaction 2. The agreement between this value and that obtained by using a second law analysis lends credence to our measured values and our assumption about the adduct geometry.

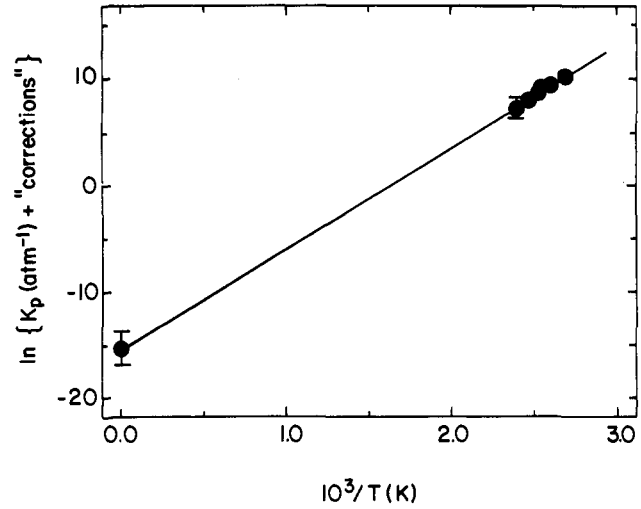

Figure 6. Modified Van't Hoff plot for the reaction of CH_3S with 1,3-butadiene. The equilibrium constants were modified as described in the text. Uncertainties are $\pm 2\sigma$.

Thermodynamic values obtained from the methods described above are in good agreement with group additivity estimates[24] for reaction 2. Previous work[14] indicates that reaction 2 exhibits no chain reaction characteristics, i.e., does not polymerize in the presence of excess 1,3-butadiene and was in the high-pressure limit with 4 Torr of SF_6 added. Our data indicate that the equilibrium constant was independent of both CH_3S and butadiene concentration, as well as total pressure. This result corroborates the data of Graham and Soltys[14] and strongly suggests that the equilibrium we observe is indeed that shown in reaction 2.

Since all the measured decays for the reaction of CH_3S with allene could be fit by a single exponential function, we conclude that no observable equilibrium was established over the temperature range studied. However, the Arrhenius plot of our data clearly exhibits curvature (see Figure 4), suggesting that simple addition to form a stable adduct may not be the only operative mechanism for the disappearance of CH_3S. Several mechanistic possibilities exist. Addition could occur at either the central carbon or the terminal carbon

$$CH_3S + H_2C{=}C{=}CH_2 \rightarrow CH_3SCH_2{=}\dot{C}{=}CH_2 \quad (7)$$

$$CH_3S + H_2C{=}C{=}CH_2 \rightarrow CH_2{=}C(SCH_3){-}CH_2{\cdot} \quad (8)$$

One might speculate that reaction 8 is more likely since the formation of an allylic-stabilized adduct favors that of the vinylic radical species, shown in eq 7. Product studies of this reaction by Griesbaum et al.[26] reveal exactly the opposite, i.e., terminal attack occurs 88% of the time at 17 °C and 95% at −75 °C. These workers invoked the unusual geometry of allene to account for this result, postulating that attack on the central carbon produces a radical that is more like a primary radical than an allylic radical because of the lack of π-orbital overlap. Rotation about the carbon–carbon bond to form an allylic stabilized radical may increase the activation energy of the process.

Another possibility is that CH_3S abstracts a H atom, especially considering the low C–H bond strength ($\leq$81.2 kcal/mol) in allene.[27] Alkyl thiyl radicals have been observed to abstract H atoms from cyclopentene and cyclohexene to give allylic-like radicals.[17] Our data indicate at least two distinct reactions occurring over the temperature range studied. It seems improbable that the two addition mechanisms described above (see eq 7 and 8) would differ in A factors by 4–5 orders of magnitude. Therefore, the disappearance of CH_3S at higher temperatures is most likely due to the abstraction of an H atom from allene. The measured Arrhenius parameters for this temperature range are consistent with values obtained for H-atom transfers involving

(22) Slagle, I. R.; Ratajczak, E.; Heaven, M. C.; Gutman, D.; Wagner, H. F. *J. Am. Chem. Soc.* **1985**, *107*, 1838. Slagle, I. R.; Ratajczak, E.; Gutman, D. *J. Phys. Chem.* **1986**, *90*, 402.

(23) The functional form is quadratic and has been calculated by using group contributions to be $\Delta C_p^\circ(T) = [5.36 - 0.0126T + (1.13 \times 10^{-5})T^2]$.

(24) Benson, S. W. *Thermochemical Kinetics*, 2nd ed.; Wiley: New York, 1976.

(25) $\Delta H_f^\circ{}_{298}(CH_3S(g)) = 31.0 \pm 1$ kcal/mol; see: Shum, L. G. S.; Benson, S. W. *Int. J. Chem. Kinet.* **1983**, *15*, 433.

(26) Griesbaum, K.; Oswald, A. A.; Qurim, E. R.; Naegele, W. *J. Org. Chem.* **1963**, *28*, 1952.

(27) Collin, J.; Lossing, F. P. *J. Am. Chem. Soc.* **1957**, *79*, 5848.

radicals with small organic molecules.[24]

The dramatic difference between the measured A factors for the addition of CH_3S to 1,3-butadiene and allene is difficult to explain. Further work on the products of these two addition reactions may be required to satisfactorily explain the observed differences.

Conclusion

We have measured the kinetics of the reactions of CH_3S with a variety of unsaturated hydrocarbons. In all cases, we observe behavior that we attribute to an addition reaction leading to a CH_3S-alkene complex. In the case of 1,3-butadiene, this complex is in equilibrium with the reactants, and we are able to extract thermodynamic information from the measured equilibrium constants. At higher temperatures, there appears to be another channel in the reaction of CH_3S with allene which we attribute to hydrogen abstraction. Because of the slow rate of reaction with simple alkenes and apparent lack of reactivity with O_2,[9] it appears that the primary fate of CH_3S in the atmosphere is reaction with NO_x.

Oxidative Dimerization of Methane over Magnesium and Calcium Oxide Catalysts Promoted with Group IA Ions: The Role of $[M^+O^-]$ Centers

Chiu-Hsun Lin, Tomoyasu Ito,[1a] Ji-Xiang Wang,[1b] and Jack H. Lunsford*

Contribution from the Department of Chemistry, Texas A&M University, College Station, Texas 77843. *Received November 26, 1986*

Abstract: The oxidative dimerization of CH_4 to C_2H_4 and C_2H_6 over MgO and CaO is strongly influenced by certain group IA ions which are employed as promoters. Lithium is an effective promoter for MgO, but sodium and potassium are not; all three group IA ions are effective promoters for CaO. Centers of the type $[M^+O^-]$ (M^+ is a substitutional group IA ion) are present in each active and selective catalyst, which supports the hypothesis that these centers are active for the formation of $CH_3^\bullet$ radicals and, therefore, in the overall oxidative dimerization reaction.

Lithium-promoted MgO is a reasonably active and selective catalyst for the oxidative dimerization of CH_4 to C_2H_6 and C_2H_4 (C_2 compounds).[2] Selectivities of 50% have been achieved at a CH_4 conversion level of 38%. The reaction is believed to occur via surface-generated methyl radicals which couple mainly in the gas phase. It has been proposed that the active sites for the formation of $CH_3^\bullet$ radicals are $[Li^+O^-]$ centers[2,3] or surface O^- ions which are in equilibrium with these centers.[4] In this paper additional evidence is given for the role of these and analogous centers of the type $[M^+O^-]$ in the activation of CH_4. (Here M^+ is a substitutional group IA ion in a group IIA oxide.) The present study also provides a comparison of the activities and selectivities which may be achieved over MgO and CaO promoted with Li^+, Na^+, or K^+ ions.

The $[M^+O^-]$ centers have been extensively studied by Abraham and co-workers[5-8] in single crystals of the host oxide. The $[Li^+O^-]$ centers exist in equilibrium with molecular oxygen at elevated temperatures and may be trapped in MgO and CaO by quenching the sample.[6] More generally, $[M^+O^-]$ centers may be formed by irradiation of the doped group IIA oxides at low temperatures. Although most of the spectroscopic work has been carried out on single crystals, $[Li^+O^-]$ centers recently have been studied in polycrystalline Li/MgO catalysts.[4]

Experimental Section

All catalysts were prepared by evaporating to dryness a slurry which contained either MgO or CaO (Aldrich, 99.999%) and the appropriate group IA carbonate. The resulting materials contained ca. 30 atomic percent alkali-metal ion, which was present mainly as the carbonate. That is, only a small fraction of the group IA ions was incorporated into the host lattice, even after activation at elevated temperatures.

The catalytic experiments were carried out in a fixed-bed flow reactor. The catalysts were dehydroxylated under flowing O_2 and then maintained in the reactant gas mixture at 700 °C for 16 h before rate data were obtained. The EPR experiments were carried out on catalysts which had reached a steady state in the flow reactor and were subsequently heated in 170 Torr of O_2 at 650 °C for 1 h before quenching. After the EPR spectra on these samples were obtained, they were warmed to 25 °C under vacuum and then irradiated (λ = 254 nm) at 77 K under 120 Torr of O_2 for 1 h.

Results and Discussion

A comparison of activity and selectivity for different combinations of group IA/group IIA oxide catalysts is given in Table I. No attempt was made to maximize yield; thus the value of 12.8% obtained for the Li/MgO catalyst is considerably less than the value of 19.4% which was obtained previously under different conditions.[2]

It is most significant that among the MgO catalysts, only Li/MgO exhibited a moderate level of conversion and selectivity, and, therefore, a relatively good C_2 yield. Although Na/MgO was a poor catlayst at temperatures <700 °C, Na/CaO was a good catalyst, which rivaled Li/MgO in C_2 yield. This observation indicates that *specific* interactions, such as the formation of $[M^+O^-]$ centers, are important in the activation of methane, at least over the range of temperatures reported here.

Evidence for the $[M^+O^-]$ centers is indeed found in the EPR spectra (Figure 1) of Li/CaO and Na/CaO, both of which gave good C_2 yields. Conversely, no $[M^+O^-]$ signal was observed in the Na/MgO and K/MgO catalysts, which did not give good C_2 yields at temperatures <700 °C. The EPR spectra of the $[M^+O^-]$ centers are characterized by $g_\parallel$ = 2.000-2.004 and $g_\perp$ = 2.054-2.109, depending on the particular group IA ion and the host oxide.[5-8] The spectrum of the $[Li^+O^-]$ center in the used

(1) (a) Permanent address: Department of Chemistry, Tokyo Metropolitan University, Tokyo 158, Japan. (b) Permanent address: Changchun Institute of Applied Chemistry, Jilin, The People's Republic of China.

(2) Ito, T.; Lunsford, J. H. *Nature (London)* **1985**, *314*, 721. Ito, T.; Wang, J.-X.; Lin, C.-H.; Lunsford, J. H. *J. Am. Chem. Soc.* **1985**, *107*, 5062.

(3) Driscoll, D. J.; Martir, W.; Wang, J.-X.; Lunsford, J. H. *J. Am. Chem. Soc.* **1985**, *107*, 58.

(4) Wang, J.-X.; Lunsford, J. H. *J. Phys. Chem.* **1986**, *90*, 5883.

(5) Abraham, M. M.; Chen, Y.; Boatner, L. A.; Reynolds, R. W. *Phys. Rev. Lett.* **1976**, *37*, 849.

(6) Chen, Y.; Tohver, H. T.; Narayan, J.; Abraham, M. M. *Phys. Rev. B: Solid State* **1977**, *16*, 5535. Olson, D. N.; Orera, V. M.; Chen, Y.; Abraham, M. M. *Phys. Rev. B: Condens. Matter* **1980**, *21*, 1258.

(7) Abraham, M. M.; Unruh, W. P.; Chen, Y. *Phys. Rev. B: Solid State* **1974**, *10*, 3540.

(8) Abraham, M. M.; Chen, Y.; Lewis, J. T.; Modine, F. A. *Phys. Rev. B: Solid State* **1973**, *7*, 2732.

0002-7863/87/1509-4808$01.50/0